© 2019. Published by The Company of Biologists Ltd | Development (2019) 146, dev171504. doi:10.1242/dev.171504

RESEARCH REPORT

Transient activity of the florigen complex during the floral transition in *Arabidopsis thaliana*

Mitsutomo Abe[1,*], Shingo Kosaka[1], Mio Shibuta[1], Kenji Nagata[1], Tomohiro Uemura[1,2], Akihiko Nakano[1,3] and Hidetaka Kaya[1,4]

ABSTRACT

FLOWERING LOCUS T (FT) is an essential component of florigen in *Arabidopsis thaliana*. Transcription of *FT* is induced in leaves, and the resulting FT protein is transported to the shoot apex, in which it initiates floral development. Previous analyses suggest that, together with the b-ZIP transcription factor FD, FT regulates the transcription of downstream targets such as *APETALA1* (*AP1*) in floral anlagen. However, conclusive *in vivo* evidence that FT is transported to the shoot apex to form an FT–FD complex is lacking. Here, using an innovative *in vivo* imaging technique, we show that the FT–FD complex and AP1 colocalise in floral anlagen. In addition, the FT–FD complex disappears soon after the floral transition owing to a reduction in *FD* transcripts in the shoot apex. We further show that misinduction of FD activity after the transition leads to defective reproductive development. Taken together, our results indicate that the FT–FD complex functions as a transient stimulus and imply that a regulatory mechanism exists during the floral transition that reduces FT–FD complex levels via modulation of *FD* expression.

KEY WORDS: *Arabidopsis thaliana*, Flowering, Florigen, FT-FD complex, *In vivo* imaging

INTRODUCTION

The timing of flowering is crucial for the reproductive success of plants. The underlying regulatory mechanism is complex, and frequently involves the integration of environmental and developmental signals to optimise the timing of flowering (Amasino, 2010; Andrés and Coupland, 2012; Huijser and Schmid, 2011; Kobayashi and Weigel, 2007; Song et al., 2015). Many plant species modulate the timing of flowering in response to changes in day length. The photoperiod-dependent flowering of *Arabidopsis thaliana* is controlled primarily by *FLOWERING LOCUS T* (*FT*) (Kardailsky et al., 1999; Kobayashi et al., 1999). Long-day conditions (LD) induce *FT* transcription in leaf phloem companion cells (Abe et al., 2015; Adrian et al., 2010; Notaguchi et al., 2008; Yamaguchi et al., 2005) and the resulting FT protein is transported to the shoot apex, in which it initiates floral development (Abe et al., 2015; Corbesier et al., 2007; Jaeger and Wigge, 2007; Notaguchi et al., 2008). There is increasing evidence that the phosphatidylethanolamine-binding protein encoded by *FT*, and the proteins that are encoded by homologous genes in other species, are essential components of a mobile floral stimulus (i.e. florigen) (Corbesier et al., 2007; Jaeger and Wigge, 2007; Lin et al., 2007; Mathieu et al., 2007; Navarro et al., 2011; Notaguchi et al., 2008; Tamaki et al., 2007).

Previous genetic and biochemical analyses have suggested that the FT protein upregulates the transcription of floral meristem identity genes, such as *APETALA1* (*AP1*), in concert with FD, a b-ZIP transcription factor, at the flanks of the shoot apical meristem (SAM) (Abe et al., 2005; Wigge et al., 2005). Anatomical analysis of *Arabidopsis* has shown that floral primordia arise after periclinal division of the cells beneath the tunica layers of the SAM (Vaughan and Polytechnic, 1955). Thus, the FT–FD complex is predicted to form and activate floral meristem identity genes in these cells. Previous studies involving FT fused to a green fluorescent protein (GFP) or 5×Myc have shown that FT moves from sieve elements to the base of the SAM (Corbesier et al., 2007; Jaeger and Wigge, 2007). However, conclusive evidence of the spatial localisation of the FT–FD complex in the SAM remains lacking.

In this study, we used an innovative *in vivo* imaging technique to reveal that FT is transported to the SAM and forms a complex with FD in specific cells beneath the tunica layers. Our imaging assays clearly show that the FT protein that is synthesised in leaves or phloem companion cells forms a functional FT–FD complex in the corpus region of the SAM and the FT–FD complex and AP1 are colocalised in floral anlagen. In addition, formation of the FT–FD complex was reduced soon after the floral induction owing to reduced *FD* expression. We also show that misinduction of FD activity during the reproductive phase leads to abnormal flower development and sterility. These results suggest that formation of the FT–FD complex is transient and that a regulatory mechanism exists during the floral transition to prevent misformation of the FT–FD complex.

RESULTS AND DISCUSSION

In vivo imaging of the FT–FD complex formation

To determine exactly where FT forms functional FT–FD complexes, we used an improved bimolecular fluorescence complementation (iBiFC) assay that involves a superfolder enhanced yellow fluorescent protein (sfEYFP) that has been engineered for efficient self-complementation (Cabantous et al., 2005; Henry et al., 2017; Kamiyama et al., 2016; Park et al., 2017; Pédelacq et al., 2006). In this assay, sfEYFP is divided into two complementary non-fluorescent fragments according to its tertiary structure: an L-fragment (a large fragment that includes the first 10 β-strands) and an S-fragment (a 17-amino-acid polypeptide that corresponds to the 11th β-strand) (Cabantous et al., 2005; Henry et al., 2017; Kamiyama et al., 2016; Park et al., 2017; Pédelacq et al., 2006). Because FT is a small (20 kDa) globular protein that may be affected by a larger tag during the transport process, we fused it to

[1]Department of Biological Sciences, Graduate School of Science, The University of Tokyo, 7-3-1 Hongo, Bunkyo-ku, Tokyo 113-0033, Japan. [2]Graduate School of Humanities and Sciences, Ochanomizu University, 2-1-1 Otsuka, Bunkyo-ku, Tokyo 112-8610, Japan. [3]Live Cell Super-Resolution Imaging Research Team, RIKEN Center for Advanced Photonics, 2-1 Hirosawa, Wako, Saitama 351-0198, Japan. [4]Department of Food Production Science, Graduate School of Agriculture, Ehime University, Tarumi, Matsuyama, Ehime 790-8566, Japan.

*Author for correspondence (mabe@bs.s.u-tokyo.ac.jp)

M.A., 0000-0002-8423-1716

Received 1 September 2018; Accepted 25 February 2019

Development (2019) 146, dev171504. doi:10.1242/dev.171504

the S-fragment to decrease the likelihood of FT transport inhibition (Fig. 1A). To evaluate whether the iBiFC assay could detect formation of the FT–FD complex *in planta*, we transiently expressed *S-FT* (which encoded FT fused to the S-fragment) and *L-FD* (which encoded FD fused to the L-fragment) in *Nicotiana benthamiana* leaf epidermal cells (Fig. 1A). iBiFC signals that indicated specific association between FT and FD were observed in the nuclei of cells that co-expressed S-FT and L-FD (Fig. S1).

To further evaluate the effectiveness of this assay, we first generated transgenic *Arabidopsis* that expressed *S-FT* under the control of the *HEAT-SHOCK PROTEIN 18.2* (*HSP18.2*) promoter (*pHSP::S-FT*) (Takahashi and Komeda, 1989) and *L-FD* under the control of native *FD* regulatory elements (*gFD::L-FD*) in the *fd-1* background (Fig. S2). Induction of *S-FT* in all tissues including SAM by whole-plant heat treatment on day 9 under LD significantly accelerated the flowering of *pHSP::S-FT; gFD::L-FD; fd-1* plants (Fig. 1B, Fig. S3). We then investigated the formation of the FT–FD complex based on iBiFC signals. Strong iBiFC signals were detected mainly in the nuclei of corpus cells of the *pHSP::S-FT; gFD::L-FD; fd-1* plants 24 h after heat treatment, whereas no sfEYFP fluorescence was observed in the SAM of heat-treated *pHSP::S; gFD::L-FD; fd-1* plants (Fig. 1C-E). In parallel with the iBiFC assay, we also analysed the spatio-temporal localisation of FD in *gFD::sfEYFP-FD; fd-1* plants (Fig. S4). The distribution of sfEYFP-FD indicated that FD was localised at the inner region of the vegetative meristem and leaf primordia (Fig. 1F). This localisation pattern was very similar to the fluorescence pattern observed in the iBiFC assay (Fig. 1D,F), which implies that FT binds to FD in the nuclei of cells in which FD is expressed.

Formation of the FT–FD complex at floral anlagen

The endogenous FT protein is transported from phloem companion cells of the leaf to the shoot apex. To monitor the iBiFC signals that are obtained from leaf-derived S-FT, we induced the expression of *S-FT* in the leaf blades of *pHSP::S-FT; gFD::L-FD; fd-1* plants by heat-pulse treatment (Fig. S5). This treatment effectively induced flowering even under non-inductive short-day conditions (SD), under which endogenous *FT* is not normally expressed (Fig. 2A,B). Weak iBiFC signals were observed mainly in the nuclei of corpus cells of *pHSP::S-FT; gFD::L-FD; fd-1* plants 24 h after heat treatment of the leaves, but iBiFC fluorescence was stronger 48 h after treatment (Fig. 2C-E). The fluorescence pattern of the iBiFC assay was very similar to that of sfEYFP-FD in the SD-grown *gFD::sfEYFP-FD; fd-1* plants (Fig. 2F). We further induced *S-FT* expression by using a *SUCROSE-PROTON SYMPORTER 2* (*SUC2*) promoter, which is active specifically in phloem companion cells (Fig. S6) (Corbesier et al., 2007; Imlau et al., 1999; Jaeger and Wigge, 2007). Expression of *S-FT* under the control of this promoter accelerated flowering under LD, and nuclear-localised iBiFC signals were again observed mainly in the corpus region (Fig. 2G,H). Taken altogether, these observations indicate that the S-FT protein that is synthesised in the leaf is transported to the SAM and forms a functional FT–FD complex in the nuclei of cells in which FD is produced.

Next, we analysed the expression of *AP1* during the initial steps of the floral transition in the transgenic plants that expressed *pSUC2::S-FT* and *gFD::L-FD*. When *pSUC2::S-FT*, *gFD::L-FD* and *gAP1::AP1-mCherry* were co-expressed, the AP1-mCherry and iBiFC fluorescence colocalised in a small group of cells in the inner region of the SAM (i.e. floral anlagen) (Fig. 2I). This colocalisation of the FT–FD complex and AP1 implies that AP1 is induced in a subset of cells in which the FT–FD complex is formed.

As mentioned above, FT-GFP expressed under the control of the *SUC2* promoter has previously been detected at the 'base' of the SAM (Corbesier et al., 2007). In the earlier study, however, *pSUC2::FT-GFP* could not fully rescue the late-flowering *ft* phenotype, and the expression of *FT-GFP* driven by a minor-veins-specific promoter could not accelerate flowering (Corbesier et al., 2007). These observations suggest that the FT-GFP protein cannot effectively function as a long-distance floral stimulus. Here, in contrast, we clearly showed that FT effectively accelerated flowering and formed an FT–FD complex in the inner region of the SAM when fused to the smaller S-fragment (Fig. 2G-I). Thus, the iBiFC fluorescence patterns likely reflect localisation of the authentic FT–FD complex in the SAM at the time of the floral transition.

Dynamics of the FT–FD complex during the floral transition

Although the importance of the florigen complex in initiating the floral transition has been established, little is known about its role during the floral transition. Interestingly, when we induced *S-FT* expression after the floral transition (day 30 under inductive LD) by whole-plant heat treatment, we could not detect the iBiFC signal in

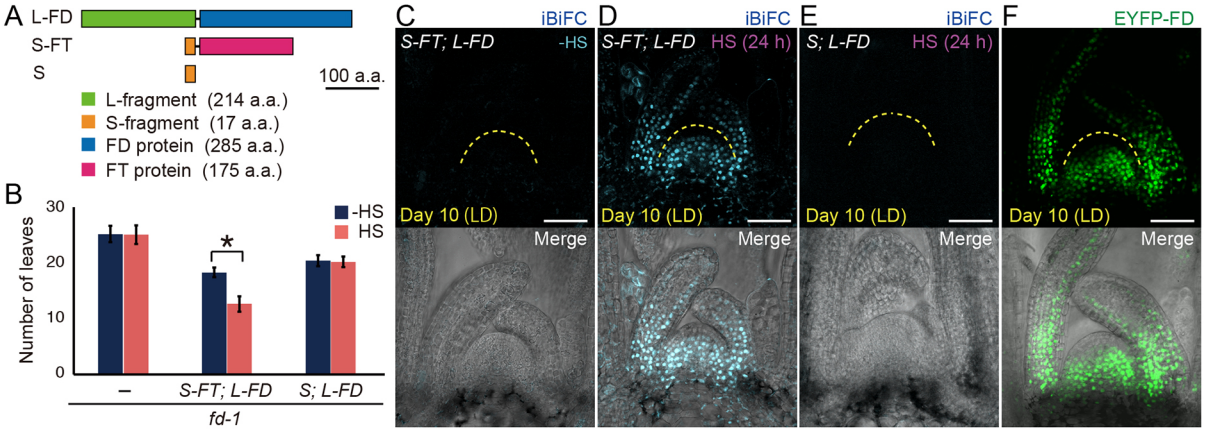

Fig. 1. iBiFC assay. (A) Diagram of the fusion proteins used in the iBiFC assay. (B) Flowering phenotypes of *pHSP::S-FT; gFD::L-FD; fd-1* plants after whole-plant heat treatment (HS) on day 9 under LD. Data are mean±s.d. (n=9). (C-E) Images from the iBiFC assay involving transgenic *Arabidopsis* plants grown under LD. Confocal images showing the shoot apex from *pHSP::S-FT; gFD::L-FD; fd-1* control (C) and heat-treated (D) plants, and *pHSP::S; gFD::L-FD; fd-1* heat-treated plants (E). Nine-day-old seedlings were heat-treated or not for 2 h and fluorescence images of the iBiFC assay were obtained 24 h after treatment. (F) Localisation of sfEYFP-FD in *gFD::sfEYFP-FD; fd-1* plants on day 10 under LD. The yellow dashed line indicates the outline of the shoot apex. *P<0.001, Student's t-test. Scale bars: 50 µm.

Development (2019) 146, dev171504. doi:10.1242/dev.171504

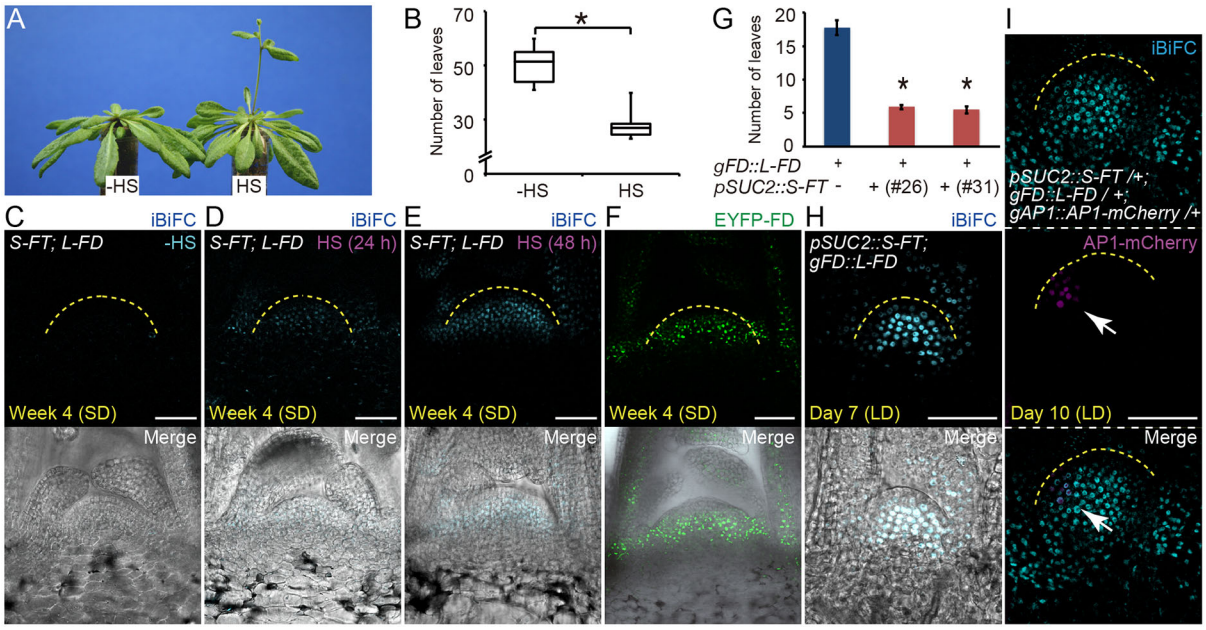

Fig. 2. Colocalisation of the FT–FD complex and AP1 at the floral anlage. (A,B) Flowering phenotypes of SD-grown *pHSP::S-FT; gFD::L-FD; fd-1* plants after the leaf blades were heated. Data are mean±s.d. ($n \geq 15$). (C-E) Confocal images from the iBiFC assay involving *Arabidopsis* plants. Longitudinal sections that show the shoot apex of *pHSP::S-FT; gFD::L-FD; fd-1* plants (grown under SD for 4 weeks) after the leaf blades underwent control (C) or heat (D,E) treatments at 24 h (D) or 48 h (C,E) after treatment. (F) sfEYFP-FD signals in *gFD::sfEYFP-FD; fd-1* plants grown under SD for 4 weeks. (G) Flowering phenotypes of *pSUC2::S-FT; gFD::L-FD; fd-1* plants. Data are mean±s.d. ($n \geq 13$). (H,I) Confocal images showing the shoot apex of *pSUC2::S-FT; gFD::L-FD; fd-1* plants grown under LD (H) and *pSUC2::S-FT/-; gFD::L-FD/-; gAP1::AP1-mCherry/-; fd-1* plants grown under LD (I). The white arrow indicates a cluster of cells expressing AP1-mCherry. The yellow dashed line indicates the outline of the shoot apex. *P<0.001, Student's t-test. Scale bars: 50 µm.

the reproductive SAM of *pHSP::S-FT; gFD::L-FD; fd-1* plants (Fig. 3A). Therefore, to characterise the temporal behaviour of the FT–FD complex during the floral transition, we monitored iBiFC fluorescence on day 5 or 7 after the artificial induction of flowering. For floral induction, we activated the *S-FT* gene in *pHSP::S-FT; gFD::L-FD; fd-1* plants by whole-plant heat treatment on day 9 under

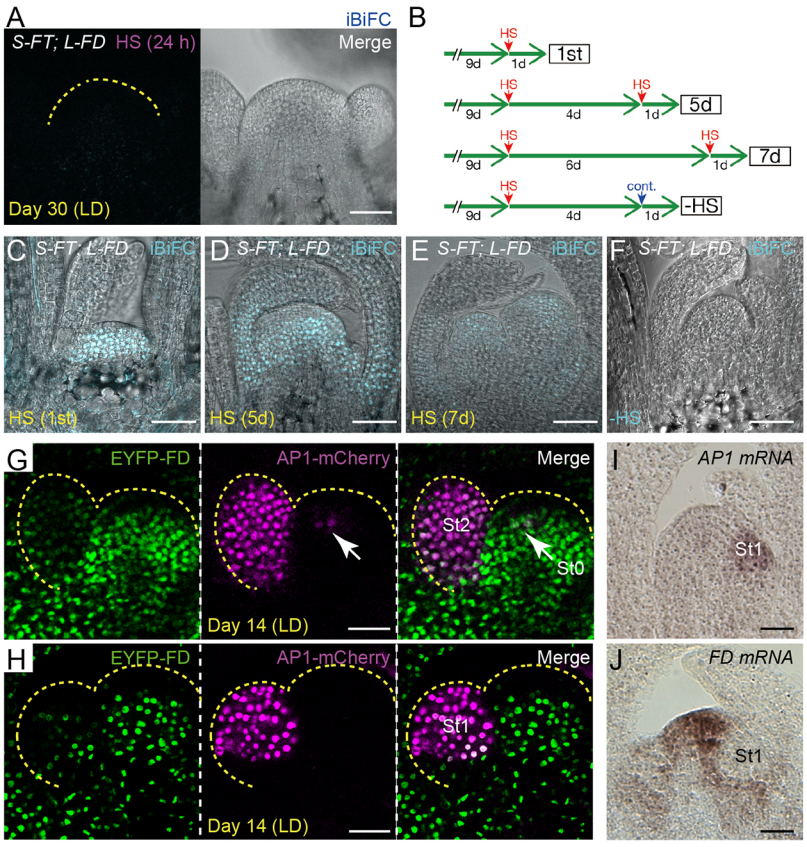

Fig. 3. Dynamics of the FT–FD complex during the floral transition. (A) Image of iBiFC signals in the reproductive SAM of whole-plant heat-treated *pHSP::S-FT; gFD::L-FD; fd-1* plants under LD. (B) Diagram showing the evaluation of FT–FD complex formation during the floral transition under LD. Arrows indicate the timing of heat-shock (HS; red) or control (cont.; blue) treatment. Samples were analysed under a microscope 24 h after the last treatment. (C-F) Images of iBiFC signals in the shoot apex of *pHSP::S-FT; gFD::L-FD; fd-1* plants. Fluorescence signals were observed at the following time points (see panel B): 1st (C), 5 days (5d; D), 7 days (7d; E) and –HS (F). (G,H) Expression of FD and AP1 during the floral transition under LD. Shown are confocal images of the shoot apex of 14-day-old *gFD::sfEYFP-FD; gAP1::AP1-mCherry; fd-1* plants. The white arrow indicates the cluster of cells expressing AP1-mCherry. (I,J) Expression patterns of *AP1* (I) and *FD* (J) during the floral transition under LD. The yellow dashed line indicates the outline of the shoot apex. St0, floral anlage; St1, stage 1; St2, stage 2. Scale bars: 50 µm.

Development (2019) 146, dev171504. doi:10.1242/dev.171504

LD. We then induced the *S-FT* gene again on day 4 or 6 after the first heat treatment to evaluate the formation of the FT–FD complex during the transition (Fig. 3B). On day 5 after the first treatment, the iBiFC signals in the primary SAM were less intense than in the vegetative SAM (Fig. 3C,D,F). Furthermore, iBiFC signals were barely detectable in the floral meristem 7 days after the first treatment (Fig. 3E). These observations suggest that the floral transition affects the effective formation of the FT–FD complex and that the SAM cannot respond to FT signals via FD after the transition.

To characterise further the dynamics of the FT–FD complex, we analysed the expression of *gFD::sfEYFP-FD* instead of the iBiFC signals during the floral transition. We observed that sfEYFP-FD colocalised with AP1-mCherry at the floral anlage, but was barely detectable in the early stages of subsequent floral meristem development (Fig. 3G,H). Furthermore, *in situ* hybridisation analysis revealed that the transcription of *FD* was greatly reduced at the floral meristem in which *AP1* was expressed (Fig. 3I,J). This result is consistent with previous reports that *FD* expression is directly repressed by AP1, which is a MADS-box transcription factor (Kaufmann et al., 2010; Winter et al., 2015). Thus, the FT–FD complex seems to disappear soon after the floral transition, likely because *FD* expression is repressed by AP1.

We also observed that sfEYFP-FD fluorescence disappeared in the primary SAM during the transition (Fig. 4A-C). Moreover, strong *pFD-GUS* activity was detected in the vegetative SAM (Fig. 4D, Fig. S7), whereas no activity was detected in the shoot apex after the floral transition (Fig. 4E, Fig. S7). Because AP1 is not expressed in the whole SAM region, it is likely that another transcription factor (or factors) is required to inhibit *FD* transcription in the primary SAM.

To gain further insight into the molecular mechanism that underlies the reduced formation of the FT–FD complex, we assessed the influence of the *fd* mutation on FT subcellular localisation. When visualised as an enhanced GFP (EGFP) fusion protein (*p35S::FT-EGFP*), FT was detected mainly in the nuclei of corpus cells in the SAM (Fig. 4F,G, Fig. S8). In the corpus cells of *p35S::FT-EGFP; fd-1* plants, however, the FT-EGFP signal was not concentrated in the nucleus (Fig. 4F,G, Fig. S8). Therefore, decreased FD activity appears to affect nuclear localisation of the FT protein and prevent the formation of a functional FT–FD complex.

AP1 and LEAFY, which are key transcription factors in the determination of floral meristem identity, are known to generate a positive-feedback loop downstream of the FT–FD complex (Liljegren et al., 1999; Schultz and Haughn, 1993). As an input signal can cause a positive-feedback loop to lock into an active state, even after the input signal is deactivated (Alon, 2007), floral meristem identity in young floral primordia is likely to be maintained even though the FT–FD complex disappears in the early stages of floral development.

Defective reproductive organs resulting from misinduction of FD

To determine whether misinduction of *FD* during the floral transition could affect reproductive development, we generated transgenic plants that expressed a dexamethasone (dex)-inducible functional construct that contained FD fused to the glucocorticoid-receptor (*p35S::FD-GR*) (Fig. S9). Application of dex to multiple *p35S::FD-GR* plant lines on days 17 and 20 after germination led to abnormal flower development and severely reduced fertility (Fig. 4H-K). Within the individual flowers, the most remarkable defect was boat-shaped sepals in the outermost whorl (Fig. 4H-J). In the second whorl, a reduction in the number and size of petals was often observed (Fig. 4J). Although the development of the stamen filaments was normal, the development of the anther was defective and the immature anther contained few

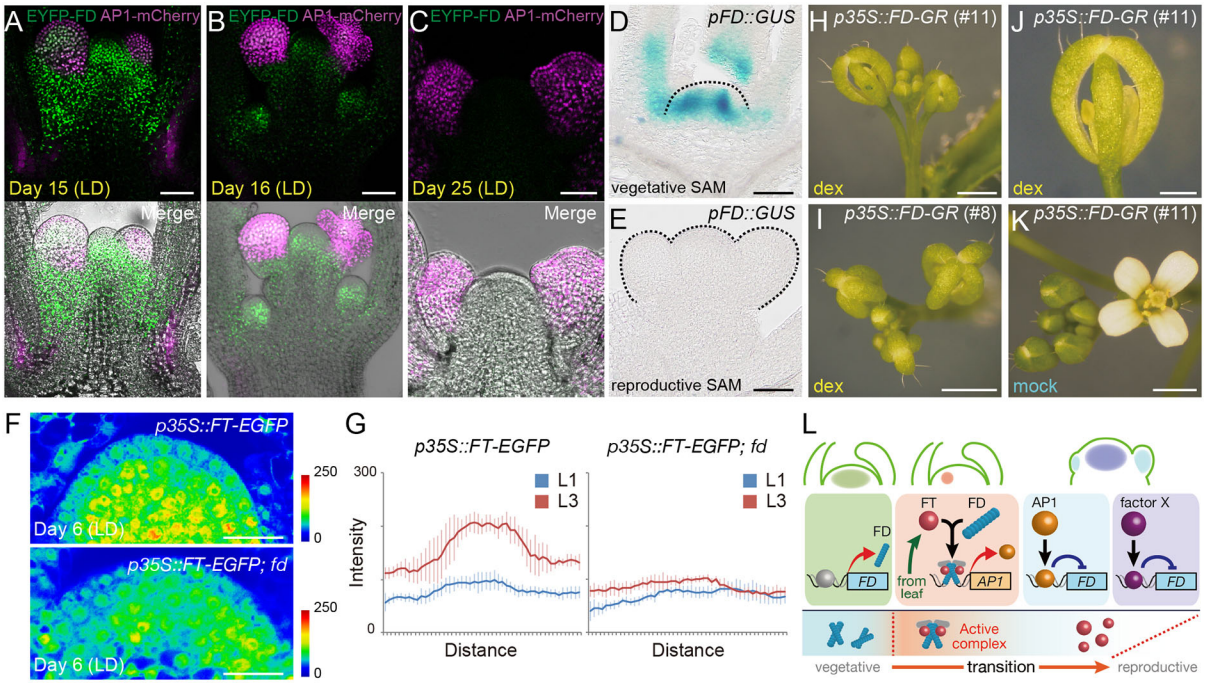

Fig. 4. Defective reproductive organs resulting from FD misinduction. (A-C) Expression of FD and AP1 during the floral transition under LD. Shown are confocal images of longitudinal sections of the shoot apex of 15-day-old (A), 16-day-old (B) and 25-day-old (C) *gFD::sfEYFP-FD; gAP1::AP1-mCherry; fd-1* plants. (D,E) Images of GUS staining in the SAM of *pFD::GUS* plants during the vegetative (D) or reproductive (E) phase. (F) Nuclear localisation of FT. Shown is the intensity of EGFP signals in longitudinal sections of the shoot apex of *p35S::FT-EGFP* and *p35S::FT-EGFP; fd-1* plants. (G) Plot of EGFP intensity in epidermal (L1) and corpus (L3) cells of *p35S::FT-EGFP* and *p35S::FT-EGFP; fd-1* plants (see Fig. S8). Data are mean±s.d. (*n*=5). (H-K) Inflorescence phenotypes of *p35S::FD-GR* plants in LD. Dex-treated inflorescence shoot (H,I), flower (J) and mock-treated inflorescence shoot (K) are shown. (L) Model of florigen complex activity during the floral transition. Black dotted line indicates the outline of the shoot apex. Scale bars: 50 µm (A-F), 1 mm (H,I,K), 500 µm (J).

Development (2019) 146, dev171504. doi:10.1242/dev.171504

pollen grains (Fig. 4J). In addition to the defects in flower development, dex-treated *p35S::FD-GR* plants formed inflorescence shoots that contained flower-like structures, which likely resulted from a loss of floral identity. These observations suggest that reduced FD activity during the early stages of the floral transition is required for normal reproductive development.

Concluding remarks

In summary, *in vivo* visualisation of the FT–FD complex using the iBiFC assay revealed that FT forms the FT–FD complex in cells that express FD, and the complex disappears owing to a reduction in *FD* levels soon after the transition in *Arabidopsis*. Furthermore, misinduction of FD after the floral transition resulted in abnormal reproductive development. Collectively, these results suggest the presence of a regulatory mechanism that prevents misformation of the FT–FD complex through the control of *FD* expression, and a distinct growth phase that is defined by the activity of the FT–FD complex (Fig. 4L). After the floral transition, the FT that is expressed in the reproductive organs is still involved in maintaining floral commitment in a non-cell-autonomous manner (Liu et al., 2014; Müller-Xing et al. 2014). Our results suggest that the FT–FD complex plays a role in floral induction, but probably not in floral commitment. The misformation of the FT-FD complex that results from misinduction of FD may affect the proper function of FT after the floral transition. Identification of other partners that mediate FT signals for floral commitment will be of great help in understanding the molecular mechanism that is involved in the transition of meristem identity during the life cycle of *Arabidopsis*.

As bZIP transcription factors are known to form homo- and/or hetero-dimers, another possible cause of abnormality in *p35S::FD-GR* is the induction of novel phenotypes through transcriptional changes in the dex-treated *p35S::FD-GR* plants following the misinduction of FD during the reproductive phase.

Although several target genes of FD have been reported (Abe et al., 2005; Wigge et al., 2005), little is known about the other downstream targets of FD. Comprehensive gene expression analysis in the tissue where the defects were observed in the dex-treated *p35S::FD-GR* will be necessary.

In rice, the localisation pattern of each component of the florigen complex and the expression of its downstream target have been reported, and the authors concluded that the florigen complex persists in the primary inflorescence meristem during the floral transition (Tamaki et al., 2015). The transition of the meristem fate during the floral transition in rice is complex and the primary SAM does not form the floral meristem directly. In contrast, the primary SAM in *Arabidopsis* directly forms the floral meristem on its flanks. Our findings regarding the dynamics of the florigen complex described here are different from those that have been previously reported in rice and are likely to reflect essential differences between the two types of inflorescence development. Future studies on the dynamics of the florigen complex in various plant species, which focus on the transcriptional regulation of *FD*, will provide further insight into the molecular mechanisms that underlie the floral transition.

MATERIALS AND METHODS

Plant materials and growth conditions

Arabidopsis mutants and transgenic plants used in this study are all in Columbia (Col) background. Transgenic plants used in this study are listed in Table S1.

For the analysis of flowering phenotypes, plants were grown on soil or Murashige and Skoog (MS) medium (Wako) supplemented with 1% sucrose at 22°C under LD (16 h light/8 h dark) or SD (8 h light/16 h dark) conditions. Flowering time was measured by counting total leaves (rosette and cauline leaves).

Plasmid construction

All PCR-generated cloning fragments used in this study were produced using PrimeSTAR GXL DNA polymerase (TaKaRa). Sequences of the primer used in the plasmid construction are shown in Table S2.

psfEYFP

For the iBiFC assay, we first synthesised the artificial *sfEYFP* gene, which obtains 15 mutations, as described by previous reports (Cabantous et al., 2005; Henry et al., 2017; Ottmann et al., 2009; Park et al., 2017; Pédelacq et al., 2006), and subcloned it into *pTAKN-2* vector (Biodynamics Laboratory).

p35S::S-FT

For the *p35S::S-FT*, the S-fragment (amplified by PCR using the primer set pRI-sfEYFP11-up1 and sfEYFP11-Ver.2-low1) and the *FT* cDNA fragment (amplified by PCR using the primer set sfEYFP11-FT-up2 and pRI-FT-low2) were cloned into the NdeI/SalI-digested *pRI201-AN* (TaKaRa) using an In-fusion HD Cloning Kit (TaKaRa).

p35S::L-FD

For the *p35S::L-FD*, the L-fragment (amplified by PCR using the primer set pRI-sfEYFP-up1 and pRI-sfEYFP1∼10-low1) and the *FD* cDNA fragment (amplified by PCR using the primer set Linker-FD-up2 and pRI-FD-low2) were cloned into the NdeI/SalI-digested *pRI201-AN* using an In-fusion HD Cloning Kit.

p35S::L-FD(T282A)

For the *p35S::L-FD*(*T282A*), the L-fragment (amplified by PCR using the primer set pRI-sfEYFP-up1 and pRI-sfEYFP1∼10-low1) and the *FD*(*T282A*) cDNA fragment (amplified by PCR using the primer set Linker-FD-up2 and pRI-FD-T282A-low2) were cloned into the NdeI/SalI-digested *pRI201-AN* using an In-fusion HD Cloning Kit.

p35S::S

For the *p35S::S*, the S-fragment (amplified from *p35S::S-FT* by PCR using the primer set pRI-sfEYFP11N-up and pRI-sfEYFP11N-low) was cloned into the NdeI/SalI-digested *pRI201-AN* using an In-fusion HD Cloning Kit.

gFD::sfEYFP-FD

To construct the *gFD::sfEYFP-FD*, the L-fragment (amplified by PCR using the primer set pRI-sfEYFP-up1 and pRI-sfEYFP-low1) and the *FD* cDNA fragment (amplified by PCR using the primer set Linker-FD-up2 and pRI-FD-low2) were cloned into the NdeI/SalI-digested *pRI201-AN* using an In-fusion HD Cloning Kit (*p35S::sfEYFP-FD*). The 5′-region of *FD* was amplified by PCR using the primer set of pBIN-FD-pro-up1 and pBIN-FD-pro-low1. The 3′-region of *FD* was amplified by PCR using the primer set of pBIN-FD-ter-up1 and pBIN-FD-ter-low1. These genomic fragments were subcloned into the HindIII/EcoRI-digested *pBI101* (*pBIgFD*). The *sfEYFP-FD* fragment was amplified from *p35S::sfEYFP-FD* using the primer set of FD-pro-BamHI-sfEYFP-up1 and FD-ter-BamHI-FD-low1 and subcloned into the BamHI site of the *pBIgFD* vector.

pHSP::S-FT

The S-FT fragment was amplified from *p35S::S-FT* using the primer set of pTTBamHI2-sfEYFP11-FT-up and pTTBamHI-sfEYFP11-FT-low and cloned into the BamHI site of the *pTT101* vector (Matsuhara et al., 2000).

gFD::L-FD

The L-FD fragment was amplified from *p35S::L-FD* using the primer set of FD-pro-BamHI-sfEYFP-up1 and FD-ter-BamHI-FD-low1 and cloned into the BamHI site of the *pBIgFD* vector.

pSUC2::S-FT

The 5′-region of *SUC2* was amplified from the Col genome using the primer set of SUC2-pro-HindIII-up and SUC2-pro-XbaI-low. This *SUC2* promoter was replaced with the *35S* promoter fragment of *p35S::S-FT*.

Development (2019) 146, dev171504. doi:10.1242/dev.171504

pSUC2::sGFP

The 5′-region of *SUC2* was amplified from the Col genome using the primer set of SUC2-pro-pENTR-5′ and SUC2-pro-pENTR-3′ and cloned into the *pENTR/D-TOPO* cloning vector (Thermo Fisher Scientific). This *SUC2* promoter was transferred to the binary vector *pGWB4* using LR recombination reactions.

gAP1::AP1-mCherry

For the *gFD::sfEYFP-FD*, the *AP1* promoter region and coding region was amplified from the Col genome using the primer set of AP1-pro-Hind-up and AP1-ORF-Kpn-low, and the *AP1* 3′-region was also amplified using the primer set of AP1-ter-Xho-up and AP1-ter-Xba-low. The *mCherry* coding region was amplified from *pmCherry-N1* (Clontech) using the primer set of mCherry-Kpn-up and mCherry-Xho-low. These three fragments were subcloned into the *pENTR/D-TOPO* vector (Thermo Fisher Scientific; *pENTR-gAP1::AP1-mCherry*). The *gAP1-mCherry* fragment was transferred to the binary vector *pHGW* (Plant Systems Biology) using LR recombination reactions.

p35S::FD-GR

To construct the *p35S::FD-GR*, the GR fragment [amplified from the *p35S::FE-GR* (Abe et al., 2015) using the primer set GR-up and GR-low] and the *FD* cDNA fragment (amplified by PCR using the primer set FD-up and FD-low) were cloned into the XbaI/SacI-digested *pBI121* using an In-fusion HD Cloning Kit.

Agroinfiltration

Agroinfiltration was performed essentially as described previously (Voinnet et al., 2003). *Nicotiana benthamiana* were grown under LD conditions at 22°C. *Agrobacterium tumefaciens* strain pMP90 that contained an appropriate plasmid was grown at 28°C and bacterial suspension was infiltrated into the abaxial air space of a leaf using a 1 ml syringe as described previously (Voinnet et al., 2003).

Plant transformation

The binary-vectors described above were introduced into *A. tumefaciens* strain pMP90 and transformed into *Arabidopsis* plants using the floral-dip method (Clough and Bent, 1998).

Heat treatment

The *S-FT* gene was under the control of the *Arabidopsis HSP18.2* promoter (Takahashi and Komeda, 1989). For the whole-plant heat treatment, plants grown on soil or MS plate were subjected to the heat treatment at 37°C for 2 h in a custom-built cabinet.

Plants, which were grown under SD conditions for 4 weeks on soil, were subjected to heat treatment on leaf blades. The leaf blade was exposed to 37°C for 2 h using heated copper plates. Detailed procedures of heat-treatment on leaf-blades are described in Fig. S5 and Notaguchi et al. (2008).

Gene expression analysis

For the RT-PCR analysis, total RNA was extracted from whole tissues of transgenic plants using TRIzol reagent (Thermo Fisher Scientific) according to the manufacturer's instructions. Total RNA was reverse-transcribed using Super Script III Reverse Transcriptase (Thermo Fisher Scientific) and used as templates for the RT-PCR analysis.

In situ RNA hybridisation was performed according to a previously described procedure (Abe et al., 2005). Tissue samples of 12-day-old wild-type seedlings were fixed in FAA (50% ethanol, 5% acetic acid and 3.7% formaldehyde), dehydrated, embedded in paraffin and sectioned at 8 µm. These sections were hybridised at 55°C and washed in 0.1× SSC at 65°C.

For the histochemical analysis of GUS staining, tissue samples were fixed in 90% acetone on ice and then incubated at 37°C with staining solution [0.5 mg/ml X-Gluc, 50 mM sodium phosphate buffer (pH 7.0), 5 mM potassium ferrocyanide, 5 mM potassium ferricyanide, 0.1% Triton X-100]. After staining, samples were cleared in a chloral hydrate solution and sectioned at 30 µm using a VT1200 vibratome (Leica).

Microscopy analysis

iBiFC or sfEYFP-FD images were observed using an LSM510 Meta confocal laser-scanning microscope (Carl Zeiss). For observation of iBiFC and sfEYFP signals, fluorescence was excited with 488 nm argon laser and emission images were monitored in the 530-600 nm range. Multi-colour observations were carried out using a LSM780 confocal microscope (Carl Zeiss). mCherry was excited at 561 nm and the emission from 598 nm to 636 nm was observed. sfEYFP fluorescence was excited at 488 nm and the emission from 517 nm to 552 nm was observed. EGFP-intensity of FT-EGFP was observed using an LSM780 microscope and was analysed using ZEN software (Carl Zeiss). Fluorescent images of at least three individuals were observed for each figure. EGFP-intensity along the diagonal of the cell was measured and the average EGFP-intensity value of five cells is shown in Fig. 4G (see also Fig. S8).

Fluorescence images of the iBiFC assay were obtained from the transgenic *Arabidopsis* plants 24 h after the heat or control treatments. Longitudinal sections (30 µm) of shoot apex were obtained using a VT1200 vibratome.

Dexamethasone treatment

For the misinduction of FD activity during the floral transition, *p35S::FD-GR* plants on day 17 and 20 after germination were sprayed with a dexamethasone solution (10 µM dexamethasone, 0.02% Silwet L-77, 0.1% ethanol). For the continuous activation of FD during the vegetative phase, *p35S::FD-GR* seedlings were treated daily, from day 5 to day 10, with a dexamethasone solution.

Acknowledgements

We thank A. Watanabe-Taneda and A. Imai for experimental assistance. We also thank H.-Y. Hirano for critical reading of the manuscript. We are grateful to laboratory members for helpful discussions. We thank T. Araki for providing transgenic *Arabidopsis* seeds.

Competing interests

The authors declare no competing or financial interests.

Author contributions

Conceptualization: M.A., H.K.; Methodology: M.A., H.K.; Validation: M.A.; Formal analysis: M.A.; Investigation: M.A., S.K., T.U., H.K.; Resources: M.A., S.K., M.S., K.N., H.K.; Writing - original draft: M.A.; Writing - review & editing: M.A., T.U., A.N., H.K.; Visualization: M.A.; Supervision: M.A., A.N.; Project administration: M.A.; Funding acquisition: M.A.

Funding

This work was supported by the Ministry of Education, Culture, Sports, Science & Technology (MEXT) [Grants-in-Aid for Scientific Research on Innovative Areas 16H01228 to M.A., Grants-in-Aid for Scientific Research (C) 26440133 to M.A.].

Supplementary information

Supplementary information available online at
http://dev.biologists.org/lookup/doi/10.1242/dev.171504.supplemental

References

Abe, M., Kobayashi, Y., Yamamoto, S., Daimon, Y., Yamaguchi, A., Ikeda, Y., Ichinoki, H., Notaguchi, M., Goto, K. and Araki, T. (2005). FD, a bZIP protein mediating signals from the floral pathway integrator FT at the shoot apex. *Science* **309**, 1052-1056.

Abe, M., Kaya, H., Watanabe-Taneda, A., Shibuta, M., Yamaguchi, A., Sakamoto, T., Kurata, T., Ausín, I., Araki, T. and Alonso-Blanco, C. (2015). FE, a phloem-specific Myb-related protein, promotes flowering through transcriptional activation of *FLOWERING LOCUS T* and *FLOWERING LOCUS T INTERACTING PROTEIN 1*. *Plant J.* **83**, 1059-1068.

Adrian, J., Farrona, S., Reimer, J. J., Albani, M. C., Coupland, G. and Turck, F. (2010). *cis*-Regulatory elements and chromatin state coordinately control temporal and spatial expression of *FLOWERING LOCUS T* in *Arabidopsis*. *Plant Cell* **22**, 1425-1440.

Alon, U. (2007). Network motifs: theory and experimental approaches. *Nat. Rev. Genet.* **8**, 450-461.

Amasino, R. (2010). Seasonal and developmental timing of flowering. *Plant J.* **61**, 1001-1013.

Andrés, F. and Coupland, G. (2012). The genetic basis of flowering responses to seasonal cues. *Nat. Rev. Genet.* **13**, 627-639.

Cabantous, S., Terwilliger, T. C. and Waldo, G. S. (2005). Protein tagging and detection with engineered self-assembling fragments of green fluorescent protein. *Nat. Biotechnol.* **23**, 102-107.
Clough, S. J. and Bent, A. F. (1998). Floral dip: a simplified method for Agrobacterium-mediated transformation of *Arabidopsis thaliana*. *Plant J.* **16**, 735-743.
Corbesier, L., Vincent, C., Jang, S., Fornara, F., Fan, Q., Searle, I., Giakountis, A., Farrona, S., Gissot, L., Turnbull, C. et al. (2007). FT protein movement contributes to long-distance signaling in floral induction of *Arabidopsis*. *Science* **316**, 1030-1033.
Henry, E., Toruño, T. Y., Jauneau, A., Deslandes, L. and Coaker, G. (2017). Direct and indirect visualization of bacterial effector delivery into diverse plant cell types during infection. *Plant Cell* **29**, 1555-1570.
Huijser, P. and Schmid, M. (2011). The control of developmental phase transitions in plants. *Development* **138**, 4117-4129.
Imlau, A., Truernit, E. and Sauer, N. (1999). Cell-to-cell and long-distance trafficking of the green fluorescent protein in the phloem and symplastic unloading of the protein into sink tissues. *Plant Cell* **11**, 309-322.
Jaeger, K. E. and Wigge, P. A. (2007). FT protein acts as a long-range signal in *Arabidopsis*. *Curr. Biol.* **17**, 1050-1054.
Kamiyama, D., Sekine, S., Barsi-Rhyne, B., Hu, J., Chen, B., Gilbert, L. A., Ishikawa, H., Leonetti, M. D., Marshall, W. F., Weissman, J. S. et al. (2016). Versatile protein tagging in cells with split fluorescent protein. *Nat. Commun.* **7**, 11046.
Kardailsky, I., Shukla, V. K., Ahn, J. H., Dagenais, N., Christensen, S. K., Nguyen, J. T., Chory, J., Harrison, M. J. and Weigel, D. (1999). Activation tagging of the floral inducer FT. *Science* **286**, 1962-1965.
Kaufmann, K., Wellmer, F., Muiño, J. M., Ferrier, T., Wuest, S. E., Kumar, V., Serrano-Mislata, A., Madueño, F., Krajewski, P., Meyerowitz, E. M. et al. (2010). Orchestration of floral initiation by APETALA1. *Science* **328**, 85-89.
Kobayashi, Y. and Weigel, D. (2007). Move on up, it's time for change–mobile signals controlling photoperiod-dependent flowering. *Genes Dev.* **21**, 2371-2384.
Kobayashi, Y., Kaya, H., Goto, K., Iwabuchi, M. and Araki, T. (1999). A pair of related genes with antagonistic roles in mediating flowering signals. *Science* **286**, 1960-1962.
Liljegren, S. J., Gustafson-Brown, C., Pinyopich, A., Ditta, G. S. and Yanofsky, M. F. (1999). Interactions among APETALA1, LEAFY, and TERMINAL FLOWER1 specify meristem fate. *Plant Cell* **11**, 1007-1018.
Lin, M.-K., Belanger, H., Lee, Y.-J., Varkonyi-Gasic, E., Taoka, K.-I., Miura, E., Xoconostle-Cázares, B., Gendler, K., Jorgensen, R. A., Phinney, B. et al. (2007). FLOWERING LOCUS T protein may act as the long-distance florigenic signal in the cucurbits. *Plant Cell* **19**, 1488-1506.
Liu, L., Farrona, S., Klemme, S. and Turck, F. (2014). Post-fertilization expression of *FLOWERING LOCUS T* suppresses reproductive reversion. *Front. Plant Sci.* **5**, 164.
Mathieu, J., Warthmann, N., Küttner, F. and Schmid, M. (2007). Export of FT protein from phloem companion cells is sufficient for floral induction in *Arabidopsis*. *Curr. Biol.* **17**, 1055-1060.
Matsuhara, S., Jingu, F., Takahashi, T. and Komeda, Y. (2000). Heat-shock tagging: a simple method for expression and isolation of plant genome DNA flanked by T-DNA insertions. *Plant J.* **22**, 79-86.
Müller-Xing, R., Clarenz, O., Pokorny, L., Goodrich, J. and Schubert, D. (2014). Polycomb-group proteins and *FLOWERING LOCUS T* maintain commitment to flowering in *Arabidopsis thaliana*. *Plant Cell* **26**, 2457-2471.
Navarro, C., Abelenda, J. A., Cruz-Oró, E., Cuéllar, C. A., Tamaki, S., Silva, J., Shimamoto, K. and Prat, S. (2011). Control of flowering and storage organ formation in potato by FLOWERING LOCUS T. *Nature* **478**, 119-122.
Notaguchi, M., Abe, M., Kimura, T., Daimon, Y., Kobayashi, T., Yamaguchi, A., Tomita, Y., Dohi, K., Mori, M. and Araki, T. (2008). Long-distance, graft-transmissible action of *Arabidopsis* FLOWERING LOCUS T protein to promote flowering. *Plant Cell Physiol.* **49**, 1645-1658.
Ottmann, C., Weyand, M., Wolf, A., Kuhlmann, J. and Ottmann, C. (2009). Applicability of superfolder YFP bimolecular fluorescence complementation *in vitro*. *Biol. Chem.* **390**, 81-90.
Park, E., Lee, H.-Y., Woo, J., Choi, D. and Dinesh-Kumar, S. P. (2017). Spatiotemporal monitoring of Pseudomonas syringae effectors via type III secretion using split fluorescent protein fragments. *Plant Cell* **29**, 1571-1584.
Pédelacq, J.-D., Cabantous, S., Tran, T., Terwilliger, T. C. and Waldo, G. S. (2006). Engineering and characterization of a superfolder green fluorescent protein. *Nat. Biotechnol.* **24**, 79-88.
Schultz, E. A. and Haughn, G. W. (1993). Genetic analysis of the floral initiation process (FLIP) in *Arabidopsis*. *Development* **119**, 745-765.
Song, Y. H., Shim, J. S., Kinmonth-Schultz, H. A. and Imaizumi, T. (2015). Photoperiodic flowering: time measurement mechanisms in leaves. *Annu. Rev. Plant. Biol.* **66**, 441-464.
Takahashi, T. and Komeda, Y. (1989). Characterization of two genes encoding small heat-shock proteins in *Arabidopsis thaliana*. *Mol. Gen. Genet.* **219**, 365-372.
Tamaki, S., Matsuo, S., Wong, H. L., Yokoi, S. and Shimamoto, K. (2007). Hd3a protein is a mobile flowering signal in rice. *Science* **316**, 1033-1036.
Tamaki, S., Tsuji, H., Matsumoto, A., Fujita, A., Shimatani, Z., Terada, R., Sakamoto, T., Kurata, T. and Shimamoto, K. (2015). FT-like proteins induce transposon silencing in the shoot apex during floral induction in rice. *Proc. Natl. Acad. Sci. USA* **112**, E901-E910.
Vaughan, J. G. and Polytechnic, C. (1955). The morphology and growth of the vegetative and reproductive apices of *Arabidopsis thaliana* (L.) Heynh., Capsella Bursa-Pastoris (L.) Medic. and Anagallis Arvensis L. *Linn. Soc. Lond. Bot.* **55**, 279-301.
Voinnet, O., Rivas, S., Mestre, P. and Baulcombe, D. (2003). An enhanced transient expression system in plants based on suppression of gene silencing by the p19 protein of tomato bushy stunt virus. *Plant J.* **33**, 949-956.
Wigge, P. A., Kim, M. C., Jaeger, K. E., Busch, W., Schmid, M., Lohmann, J. U. and Weigel, D. (2005). Integration of spatial and temporal information during floral induction in *Arabidopsis*. *Science* **309**, 1056-1059.
Winter, C. M., Yamaguchi, N., Wu, M.-F. and Wagner, D. (2015). Transcriptional programs regulated by both LEAFY and APETALA1 at the time of flower formation. *Physiol. Plant.* **155**, 55-73.
Yamaguchi, A., Kobayashi, Y., Goto, K., Abe, M. and Araki, T. (2005). TWIN SISTER OF FT (TSF) acts as a floral pathway integrator redundantly with FT. *Plant Cell Physiol.* **46**, 1175-1189.